J Bioenerg Biomembr (2012) 44:559–569
DOI 10.1007/s10863-012-9458-8

Monitoring of real changes of plasma membrane potential by diS-C_3(3) fluorescence in yeast cell suspensions

Jaromír Plášek · Dana Gášková · Hella Lichtenberg-Fraté · Jost Ludwig · Milan Höfer

Received: 18 May 2012 / Accepted: 21 June 2012 / Published online: 19 July 2012

Abstract The fluorescent dye 3,3′-dipropylthiadicarbocyanine, diS-C_3(3), is a suitable probe to monitor real changes of plasma membrane potential in yeast cells which are too small for direct membrane potential measurements with microelectrodes. A method presented in this paper makes it possible to convert changes of equilibrium diS-C_3(3) fluorescence spectra, measured in yeast cell suspensions under certain defined conditions, into underlying membrane potential differences, scaled in the units of millivolts. Spectral analysis of synchronously scanned diS-C_3(3) fluorescence allows to assess the amount of dye accumulated in cells without otherwise necessary sample taking and following separation of cells from the medium. Moreover, membrane potential changes can be quantified without demanding calibration protocols. The applicability of this approach was demonstrated on the depolarization of *Rhodotorula glutinis* yeast cells upon acidification of cell suspensions and/or by increasing extracellular K^+ concentration.

Keywords Yeast · Fluorescent probe · Plasma membrane potential · Real changes of · Spectral analysis

Introduction

Membrane potential is a sensitive parameter of cell vitality. Therefore, the quantitative assessment of its value, and/or its changes in time belongs to the most important tasks of biophysics. This task becomes increasingly difficult as the size of examined cells decreases, in particular, when dealing with microbial cell suspensions. Direct measurement of membrane potentials is possible with glass microelectrodes (Ling and Gerard 1949; Sundelacruz et al. 2009; Ullrich et al. 1984). However, in the case of microbial cells such as yeast the use of glass microelectrodes becomes extremely tedious not only due to their small size but also to severe difficulty to immobilize them (Bakker et al. 1986; Hofer and Novacky 1986). Moreover, adding an agent to or changing the suspending medium during an experiment is almost impossible.

Membrane potentials can also be estimated indirectly by measuring the redistribution of small lipophilic ions from a suspension medium into the suspended cells following the Nernst equation. For example, a small lipophilic cation, tetraphenylphosphonium (TPP^+), has often been used as indirect marker of cell membrane potential (Hockings and Rogers 1996; Hofer and Kunemund 1985). Because of numerous technical shortcomings, TPP^+ is now mainly used as a probe of membrane potential in isolated mitochondria (Cossarizza et al. 1996; Labajova et al. 2006), while for whole-cell assays fluorescent probes have been generally preferred, as documented in many papers (e.g., Bashford 1981; Gross and Loew 1989; Pena et al. 2010; Przybylo et al. 2010; Shapiro 1994; Waggoner 1976) and several comprehensive reviews (Cohen and Salzberg 1978; Plasek and Sigler 1996; Smith 1990; Waggoner 1979).

Most of fluorescent probes, which are small lipophilic ions (usually categorized as redistribution or slow dyes), respond to actual membrane potentials by corresponding intracellular dye accumulation that equilibrates within minutes. The fluorescence response of intracellularly accumulated dye is based on changes in its spectrofluorometric parameters due to dye binding to cytosolic components (mostly proteins) and/or fluorescence quenching due to the

J. Plášek (✉) · D. Gášková
Faculty of Mathematics and Physics, Charles University in Prague, Prague, Czech Republic
e-mail: plasek@karlov.mff.cuni.cz

H. Lichtenberg-Fraté · J. Ludwig · M. Höfer
Institute of Cellular and Molecular Botany, University of Bonn, 53115 Bonn, Germany

formation of intracellular dye aggregates. The latter effect, which is common for dipropylthiacarbocyanine dyes, is pronounced in experimental protocols using high dye concentrations (Hoffman and Laris 1974; Kaji 1993; Pena et al. 2010; Sims et al. 1974). Such a complex behavior of slow dye fluorescence in cell suspensions led in the past to different and frequently contradictory reports on its responses to membrane potential changes (Plasek and Sigler 1996).

The risk of ambiguous results can be significantly reduced when working with sufficiently low dye concentrations, and evaluating the shape and other characteristics of fluorescence spectra instead of measuring only plain fluorescence intensity (Plasek et al. 1994). If quantitative information on dye accumulation in cells is not an essential requirement, it is possible to determine a mere shift of emission maximum $\left(\lambda_{\max}^{em}\right)$, and use these data as qualitative characteristics of membrane potential changes, as was reported for yeast cells (Gaskova et al. 1998; Maresova et al. 2006). Contrary to fluorescence intensity the $\left(\lambda_{\max}^{em}\right)$ shift is less affected by probe binding to cuvette walls and possible photobleaching. Though spectral measurements do not permit continuous recording of dye fluorescence changes they still enable so frequent measurements that continuity can be mimicked. A worthy alternative to tracking the membrane potential changes in cell suspensions with $\left(\lambda_{\max}^{em}\right)$ is the ratiometric method introduced by Maresova et al. (Maresova et al. 2009).

While both the above methods are suitable for qualitative monitoring of membrane potential changes, they do not permit to estimate the absolute size of these changes. For this purpose more laborious analysis of diS-C_3(3) fluorescence spectra measured in cell suspensions must be performed. Plasek and coworkers developed earlier a procedure for quantitative assessment (in mV) of membrane potential changes in animal cell lines, which is based on differences in spectral properties of the extracellular free and the intracellular bound dye fluorescence (Plasek et al. 1994). By spectral unmixing of measured fluorescence spectra F(λ) this approach yielded the ratio of bound (intracellular) to free (in cell medium) dye fluorescence intensities (B/A ratio—cf. Materials and Methods). For sufficiently low dye concentrations, the B/A ratio could be used to gauge underlying ratios of dye concentrations, which were finally related to cell membrane potential through the Nernst equation. To make the spectral analysis of diS-C_3(3) fluorescence more reliable, the so called synchronous fluorescence spectroscopy (SFS) was used, which involves the registration of the fluorescence intensity while simultaneously scanning both fluorescence excitation and emission wavelengths, keeping the wavelength difference between them constant (Lloyd 1971; Plasek et al. 2000).

The main aim of this study was to extend the existing theory of diS-C_3(3) fluorescence response to membrane potential to a more general model applicable to microbial cells, particularly to yeast cells. In yeast, the intracellular accumulation of cationic dye is severely affected by both the existence of cell wall and the activity of multidrug resistance pumps, two important features which were not considered in the previous assays (Plasek et al. 1994, 2000). An amended theoretical model for quantitative assessment of membrane potential changes in yeast cells is presented in the Appendix. The reproducibility of experimentally obtained data was demonstrated by using the aerobic yeast *Rhodotorula glutinis*. This yeast was chosen since the plasma membrane potential and its dependence on external pH were characterized earlier (Hauer and Hofer 1978; Hofer and Kunemund 1985; Hofer et al. 1985).

A significant advantage of the proposed procedure lies in the possibility to monitor the changes of intracellular dye concentration, which is necessary for calculation of membrane potentials across the plasma membrane, without separation of the cells from the medium, cell extraction and extract analyses. Moreover, the changes of membrane potential can be quantified without demanding a calibration protocol. The procedure allows for (i) a semi-continuous monitoring of membrane potential in time and quantification of its changes in the scale of mV, and (ii) a quantitative assessment of plasma membrane hyper-or depolarization when yeast cells are transferred from one to another physiological state. The latter can be done by measuring the dye fluorescence after a certain time period necessary for the new steady-state equilibrium of dye redistribution following the application of external stimuli, e.g., by changing external ion composition.

Materials and methods

Materials

Fluorescent probe diS-C_3(3), 3-propyl-2-[3-[3-propyl-2(3H)benzothiazolylidene]-1-propenyl]benzothiazolium iodide (often abbreviated as 3,3′-dipropylthiadicarbocyanine iodide), CAS no. 53336-12-2, see Scheme 1, was purchased from Fluka, and added to cell suspensions from a 20 μM stock solution in ethanol. Ethyl alcohol for UV spectroscopy, citric acid and D-glucose were from Penta (Czech Republic); yeast extract and potassium chloride from Fluka; disodium phosphate, choline chloride, peptone, MES hydrate and triethanolamine (TEA) from Sigma-Aldrich. All these chemicals were of p.a. quality, except of peptone (Cell Culture Tested), MES hydrate (Biotech. Performance Certified) and TEA (Ultra, >99.5 %).

Yeast strains, growth and manipulation

Aerobic yeast *Rhodotorula glutinis* (Rhodosporidium toruloides), ATCC 26194, was pre-cultured in YEPG medium (1 % yeast extract, 1 % peptone, 2 % glucose) at 30 °C for

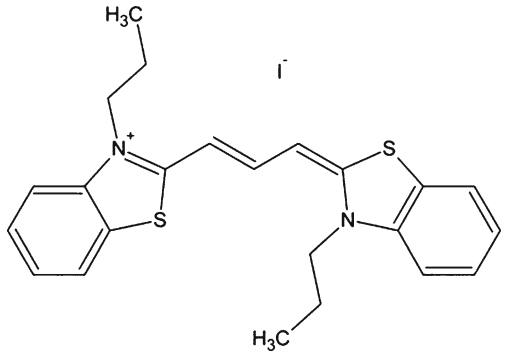

Scheme 1 Chemical structure of diS-C_3(3), CAS 53336-12-2. Note: This substance can easily be mistakenly regarded as identical with the more popular carbocyanine dye diS-C_3(5), CAS 53213-94-8, since these two similar dyes share the same abbreviated chemical name 3,3′-dipropylthiadicarbocyanine iodide

24 h. An inoculum of 150 μl was added to 20 ml fresh YEPG medium and the main culture was grown for another 20 h. Cells were harvested and washed twice by centrifugation first with distilled water and then either in citrate-phosphate (CP) buffer or in MES-TEA buffer (see below). Within 30 min after the last washing, the cells were resuspended in the respective buffer (OD ≈ 0.2–0.4 at 580 nm) containing 2 % glucose, hand-shaken, and left in this medium for 4 min before staining with diS-C_3(3). Moderate ionic strength citrate-phosphate buffer (30 mM Na_2HPO_4 and 8.8 mM citric acid, pH 6.0) was used in experiments aimed to assess the effects of both extracellular pH and external ionic strength on cell membrane potential. Acidity of cell suspensions was increased by adding adequate amounts of 0.5 M HCl. Actual pH values of all cell suspensions were directly measured with a pH-meter (inoLab pH 720 with SenTix 81 electrode, WTW, Germany). In studies focused on the role of medium ionic strength on the diS-C_3(3) fluorescence, a series of CP buffers (pH=6.0) of varying concentrations from 10 to 100 mM was prepared. Experiments towards cell depolarization by K^+ were performed with cells suspended in MES-TEA buffer (25 mM MES, pH 6.2) to avoid interference with Na^+. Cell suspensions were prepared and kept in disposable 1×1 cm UV-grade fluorometric cuvettes (Kartell, Italy). Autofluorescence spectrum of each sample was measured before adding diS-C_3(3). Upon adding the dye (20–60 nM, see figure legends), the sample was left under occasional hand-shaking to equilibrate for 18 min. Finally, the SFS spectrum of the stained cell suspension was measured. In experiments aimed to monitor the time-course of dye accumulation in cells the SFS spectra were collected every 0.5–2 min. Both the concentration of dye added to cell suspensions and the period of staining were chosen in accordance with results presented in Chapter 3.1.

Synchronous fluorescence spectroscopy (SFS) and spectral unmixing

SFS spectra were measured using Fluoromax-3 spectrofluorimeter (Jobin-Yvon Horiba), at 13 nm offset between λ_{exc} and λ_{em}, with slit widths of 2.3 nm. For the heuristic determination of reference spectra of bound dye increments of 1 nm were used (see Results and Discussion). However, such a high density of data points is not necessary for the spectral unmixing itself. Therefore, the SFS spectra of the probe fluorescence response in yeast cell assays with much larger increments of 5 nm were recorded, while keeping the slit widths still at 2.3 nm. Then the SFS spectra measured across the λ_{exc} spectral range of 520–590 nm comprised of only 15 spectral data points. To improve signal-to-noise ratio, each spectrum was measured 7 times with the integration time set to 0.5 s, and immediately averaged. Such an averaged spectrum could be obtained in 75 s, which is fast enough for monitoring membrane potentials in multiple samples in extensive titration experiments. When the kinetics of dye accumulation in yeast cells was a central point of interest, the above averaging was omitted and thus, the SFS spectra could be collected every 30 s.

The spectral unmixing of experimental SFS spectra F(λ), which means fitting F(λ) with the equation

$$F(\lambda) = AF_F(\lambda) + BF_B(\lambda)$$

where $F_F(\lambda)$ and $F_B(\lambda)$ are the peak-normalized basis spectra of free and bound dyes found by the method of trials and errors described in (Plasek et al. 2000), and A and B are coefficients determining their respective abundances in the mixed spectrum F(λ). This fitting was performed using the Nonlinear Regression module of SigmaPlot 11 software (Systat Software Inc., USA), with a user-defined equation $f = a * x + b * y$ added to the Regression Wizard. With a specially designed macro it was possible to convert spectral data from 6 to 8 samples to final membrane potential differences in about 20 min. Note that before unmixing, all raw F(λ) spectra must be corrected for cell autofluorescence, which should be measured for each sample prior to adding diSC_3(3) to the examined cell suspension.

Results

Linearity of probe fluorescence response and the time-course of diS-C_3(3) accumulation in R. glutinis cells

There are two key requirements to be considered when designing experimental protocols aimed at the assessment of membrane potential changes between two physiological states of examined cell suspensions (see also the Appendix).

First, the direct proportionality between c_{bound} and c_{in} has to be proved in advance, and second, the period of cell staining has to be adequate to allow for steady-state dye redistribution. The first requirement is not violated over the range of dye concentrations added to cell suspensions for which the fraction of bound-dye fluorescence in measured diS-C_3(3) spectra is proportional to the total dye concentration in the suspension. Results of a corresponding test with *R. glutinis* suspended in CP buffers of increasing concentrations are shown in Fig. 1. In 10 mM (low ionic strength) CP buffer, a deviation from linearity was found at dye concentrations above 20 nM. This value represents a limiting dye concentration that can be used for staining cell suspensions in 10 mM CP buffer. In both 30 mM (moderate) and 100 mM (high ionic strength) CP buffers corresponding critical diS-C_3(3) concentrations were significantly higher (<100 nM).

The typical time-course of diS-C_3(3) accumulation in *R. glutinis* cells (measured at room temperature, ≈ 22 °C) is shown in Fig. 2. In these dye-accumulation assays, which are necessary for determination of the time period needed for reaching the steady-state equilibrium of dye redistribution, the SFS spectra of diS-C_3(3) fluorescence were acquired without averaging multiple fluorometer runs. Then the time required for measuring a single spectrum, which is used for the assessment of the B/A ratio (the abundance coefficients of bound and free dyes, see above), was 12 s. This time is short enough, compared to the time-scale of diS-C_3(3) accumulation in cells, to eliminate possible artefacts due to a distortion of SFS spectra measured under the condition of rapidly changing fluorescence intensity during dye accumulation.

The curve shown represents the ratio of the respective diS-C_3(3) fluorescence intensities of intracellular bound dye

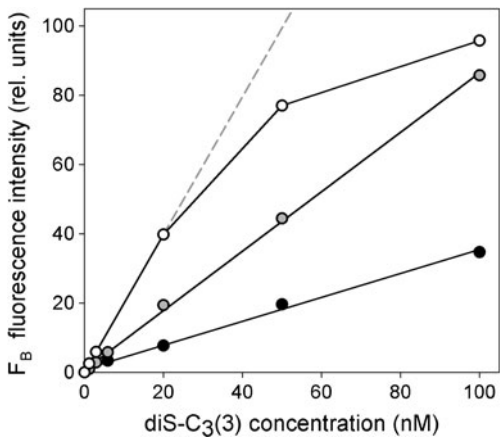

Fig. 1 Dependence of bound-dye fluorescence intensity F_B on the total concentration of diS-C_3(3) in *R.glutinis* suspensions in CP buffers (pH 6.0; cell suspension density OD=0.3). *Empty circles*—10 mM Na_2HPO_4 +2.9 mM citric-acid; *grey circles*—30 mM Na_2HPO_4+8.7 mM citric-acid, *black circles*—100 mM Na_2HPO_4+29 mM citric-acid

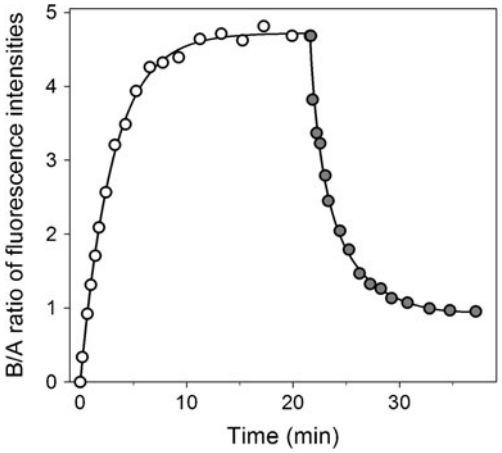

Fig. 2 Time-course of diS-C_3(3) accumulation in yeast cells (*empty circles*) and subsequent release of the dye from depolarized cells due to acidification of the cell suspension (*gray circles*) in CP buffer from pH 6.0 to pH 3.3 by addition of 0.5 M HCl at 22 min; OD_{580}=0.3, 20 nM diS-C_3(3). Data shown are representative of 3 independent experiments

and of the free dye in the cell suspension, as revealed by the B/A values resulting from spectral unmixing of experimental SFS spectra of the cell suspension. It indicates that the equilibrium dye accumulation in cells was reached within 15 min. In addition, the descending part of the curve indicates that the fluorescence response to depolarization of *R. glutinis* cells upon acidification of the cell suspension was comparably fast.

Depolarization of *R. glutinis* cells by acidification of cell medium

Washed cells were suspended in 30 mM CP buffer (pH 6) containing 2 % glucose, as described in Materials and Methods, and incubated for 4 min before adding diS-C_3(3). Depolarization experiments were started by the addition of various amounts of 0.5 M HCl resulting in different final pH value from 5.5 to 2.8. In total, data from more than 10 depolarization experiments were acquired. Since the main purpose of these depolarization experiments was not an assay on cell physiology, but the demonstration of feasibility of quantitative evaluation of diS-C_3(3) fluorescence response to membrane potential changes in yeast cells, we intentionally varied some parameters of repeated experiments, such as dye concentration, cell suspension density, and the duration of cell growth (ranging from late exponential to late stationary phase).

In accordance with the theory presented in the Appendix, a certain reference state is needed for the quantification of pH-induced cell depolarization in units of mV. The natural choice was the membrane potential of resting cells before the addition of HCl. Because the membrane potential shifts during cell depolarization from higher negative to less

negative values, the calculated values of depolarization were plotted as positive numbers. The curves shown in Fig. 3 were measured in samples containing yeast cells harvested after 20 to 35 h of growth. The density of examined cell suspensions varied from OD 0.3 to 0.4, and the final diS-C_3(3) concentration from 15 to 60 nM. Despite the mentioned variations in cell density and dye concentrations the depolarization values shown in Fig. 3 were fairly reproducible. However, when the cell depolarization induced by acidification was measured in MES/TEA buffers without glucose values about 30 % higher were obtained (data not shown).

Each set of depolarization experiments comprised 5 fully identical cell suspensions. The comparison of their SFS spectra of diS-C_3(3) fluorescence measured immediately before adding HCl was used as an additional criterion for evaluation of the robustness of experimental protocol and of data reproducibility. Relative standard deviations of mean B/A values obtained under these circumstances were of the order of 1 %.

Depolarization of *R. glutinis* yeast by increasing extracellular K^+ concentration

Similarly to cell depolarization by acidification, the membrane potential of *R. glutinis* is sensitive to K^+ concentration in suspension media, as well. The common feature of experiments focused to depolarization of *R. glutinis* cells by increasing extracellular K^+ concentration was their ability to maintain the membrane potential practically constant up to outside KCl concentrations of 10 mM. At higher KCl concentrations a significant cell depolarization was observed, Fig. 4, which increased linearly with the logarithm of KCl concentrations. The slope of the depolarization line was about 53 mV, close to the Nernstian value of 59 mV, indicating rather high plasma membrane permeability for K^+. The ability of *R. glutinis* cells to maintain membrane polarization at low outside potassium concentrations is obviously due to electrical compensation of the moderate influx of positive charges by corresponding proton extrusion through the plasma membrane H^+-ATPase.

Effects of the ionic strength of cell suspension media on diS-C_3(3) accumulation in *R. glutinis* cells

The effect of medium ionic strength, as described in the Appendix, was tested using a series of CP buffers of following concentrations: 10, 20, 30, 50, 75 and 100 mM Na_2HPO_4 with proper amounts of citric acid to give pH 6.0. All samples contained equal density of suspended cells (OD=0.32). The rest of the experimental protocol was as described in Materials and Methods.

With increasing buffer concentration, which is roughly proportional to the cell medium ionic strength, a significant decrease in the B/A ratio of diS-C_3(3) fluorescence spectra of cell suspensions was found—Fig. 5. Such a decrease mimicks a regular response of diS-C_3(3) fluorescence to cell depolarization. Therefore, the B/A dependence on the buffer concentration can also be plotted as a "false" membrane depolarization when calculated using Eq. A3, which ignores the effect of surface potential represented in equation Eq. A7. Compared to buffer with the lowest ionic-strength (10 mM), the false cell depolarization in 100 mM CP buffer comprised up to 44 mV. Similar results of "false" cell

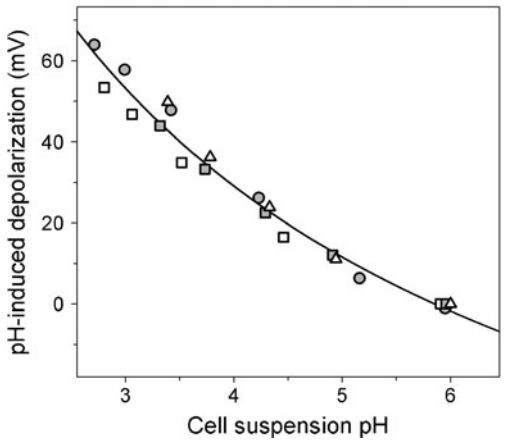

Fig. 3 Depolarization of *R. glutinis* cells by medium acidification with various volumes of 0.5 M HCl. Membrane potential of cells suspended in CP buffer of pH 6.0 was taken as the reference state for calculation of cell depolarization. *Full circles* (OD=0.38, 15 nM diS-C_3(3), cells grown for 20 h); *squares*, both empty and full, (OD=0.44, 50 nM diS-C_3(3), measured on the same day after 30 h of growth); *triangles* (OD=0.37, 60 nM diS-C_3(3), cells grown for 35 h). The *line* represents the least-squares fit to the full set of data points obtained in four independent experiments. All cell suspensions were prepared in 30 mM CP buffer

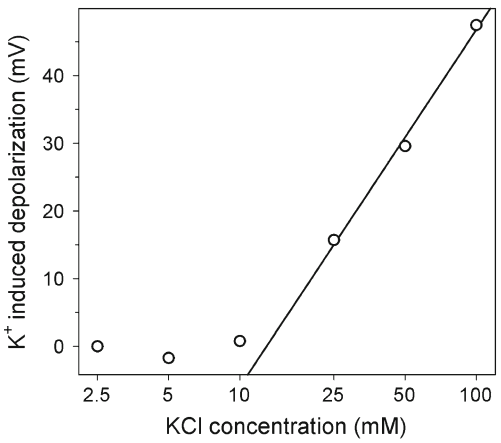

Fig. 4 Depolarization of *R. glutinis* cells following the addition of various amount of KCl to the suspension medium (25 mM MES-TEA buffer with 2 % glucose, pH 6.2, diS-C_3(3) concentration 20 nM, cell suspension density OD=0.22). Membrane potential of cells suspended in 2.5 mM KCl medium (was taken as the reference state for calculation of cell depolarization. *Full line* is a linear regression fit to data corresponding to the three highest KCl concentrations. Data shown are representative of 3 independent experiments

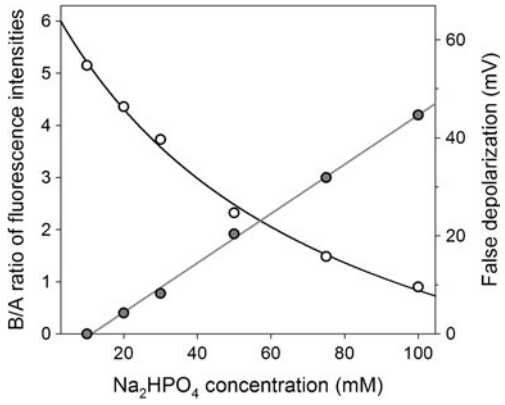

Fig. 5 Effect of ionic strength of cell suspensions on the accumulation of diS-C_3(3) in *R. glutinis* cells (suspension density OD=0.32). *Empty circles*—B/A ratios calculated from the SFS spectra of diS-C_3(3) fluorescence. *Full circles*—corresponding false cell depolarization (in mV), diS-C_3(3) fluorescence measured in 10 mM CP buffer was taken as the reference state

depolarization were obtained also with MES-TEA buffer (not shown).

CP buffer of moderate concentration (30 mM) was used throughout the experiments presented in this paper because at that buffer concentration the respective intensities of diS-C_3(3) fluorescence due to free dye in the suspension medium and bound dye accumulated in cells were both reasonably high and of comparable magnitudes.

Discussion

The use of cyanine dyes as fluorescent probes for assessment of the electrical potential differences across biological membranes has been documented in numerous publications, cf. Introduction. The reproducibility of obtained results was significantly increased by application of the red shift in fluorescence emission spectra of intracellularly bound dye (Gaskova et al. 1998; Maresova et al. 2006). This approach made it possible to reduce errors due the fluctuation of raw fluorescence intensities caused by, e.g., binding of fluorescent probe molecules to cuvette walls. The innovative aspect of the method presented in this paper consists in the advanced use of our earlier finding (Plasek et al. 1994), and its application to yeast cells. The authors demonstrated that that the amount of dye bound to intracellular components, mostly proteins, is proportional in certain limited range to the outside dye concentration. Once the amount of intracellular bound dye is in a dynamic equilibrium with intracellular free dye concentration, the latter (which is directly related to the membrane potential) can be assessed from the amount of bound dye measured by the spectral analysis of emitted fluorescence. The theoretical background of this procedure is given in the Appendix.

Although the presented approach, as any other previously published procedure, cannot yield membrane potentials in absolute units of mV it allows to quantify membrane potential changes induced by external stimuli, e.g., by changing the ionic composition of the cell surroundings. In addition, the seemingly complicated spectroscopic approach appears to be superior to protocols based on cumbersome, and often uncertain, calibration of fluorescence intensity response to experimentally caused membrane potential changes, such as treatment of cell suspensions with valinomycin in the presence of varying [K^+] concentrations (Ehrenberg et al. 1988; Freedman and Hoffman 1979; Hladky and Rink 1976; Hoffman and Laris 1974; Kaji 1993; Mao and Kisaalita 2004; Sims et al. 1974). A special advantage of the present procedure consists in the abolition of the otherwise necessary sample taking and following separation of cells from the medium. This makes possible a semi-continuous recording of cell suspension fluorescence as a measure of membrane potential, interrupted only for short periods (tens of seconds) needed for emission spectra measurements.

In order to validate this procedure we used the yeast *Rhodotorula glutinis*, in which the plasma membrane potential had been plausibly assessed by using lipophilic ions (Hauer and Hofer 1978; Hauer et al. 1981; Hofer and Kunemund 1985). The published results indicated a strong depolarization of the plasma membrane by increasing external concentration of both H^+ and K. Figures 3 and 4 depict corresponding cell depolarization assessed by the present procedure in units of mV. Actually, the individual slope of depolarization lines in the two figures each indicates the membrane permeability to the respective cation. In *R. glutinis*, the slopes of depolarization lines were 11–26 for H^+ and 53 mV for K^+. Hence, they could be used to characterize the plasma membrane permeability for K^+ in respect to the occurrence of a particular transport system in corresponding deletion mutants. Unfortunately, such mutants are not available for *R. glutinis*. Experiments with transport deficient mutants of *Saccharomyces cerevisiae* are in progress.

The cell depolarization by K^+ started at outside K^+ concentrations higher than 10 mM. This indicates that at lower K^+ concentration the moderate influx of K^+ can be electrically compensated by increased H^+ extrusion through the plasma membrane ATPase. Only at K^+ concentrations above 10 mM the effect of K^+ influx cannot be further compensated by the ATPase and consequently the inward flow of positive charges leads to cell depolarization. In a similar way, increasing outside H^+ concentration also effected significant cell depolarization. The slope of the depolarization line varied from 11 mV at pH 6-5 to 26 mV at pH 4-3. The different slopes of depolarization lines for the two cations document significantly lower plasma membrane permeability to H^+ as compared with K^+.

Following the theory presented in the Appendix, the amount of bound dye should depend significantly on the ionic strength of cell suspension medium. Indeed, with increasing ionic strength the amount of dye bound was decreased. This is consistent with the fact that cell surface potential is reduced with increasing ionic strength. Reducing cell surface potential brings about lowering of dye concentration in the close proximity to the cell membrane and thus, leads to the observed "false" cell depolarization, as shown in Fig. 5. On the other hand, the amount of dye accumulated in cells significantly increases in buffers of low ionic strength. Hence, to match the requirements of proportionality between diS-C_3(3) fluorescence and the amount of dye accumulated in cells it is necessary to use low extracellular dye concentrations (cf. Fig. 1). Buffer and dye concentrations used in the present study (i.e., 30 mM CP buffer or 25 mM MES-TEA and 40 nM diS-C_3(3)) satisfy well this crucial requirement of the experimental protocol.

General principles to be respected when designing experimental protocols can be deduced from the Appendix. The low standard deviation of the B/A ratios (about 1 %) measured in repeated experiments with cell suspensions of various densities and dye concentrations (Fig. 3) provided evidence for the robustness of the present procedure. Note, however, that while the present procedure proved to be very powerful for measuring changes of membrane potential in individual cell suspensions, it cannot be used for the assessment of membrane potential differences between different yeast strains nor between cell cultures grown under different conditions. Another shortcoming may be the proper choice of the reference state for assessment of membrane potential change. For example, in case of membrane depolarization measurements, the reference state should correspond to conditions under which the highest stable membrane potential can be expected.

Acknowledgments Supported by Research Grant MSM 0021620835, and Czech Science Foundation grant 205/10/1121, as well as by BMBF under the SysMO (System Biology of Microorganisms) ERA-Net grant 03 3982 B. We also thank Iva Benesova for her assistance in growing yeast cell cultures and experimental support.

Appendix

Theory of diS-C_3(3) fluorescence response to membrane potential changes in yeast

Implications of the Nernst equation (Plasek et al. 1994)

The standard interpretation of the relationship between membrane potential and the uptake of small lipophilic ions by cells and/or cell organelles is based on the assumption that the equilibrium concentrations of unbound ions in cells, c_{in}, and cell suspension medium, c_{out}, obey the Nernst equation (Ehrenberg et al. 1988; Krasznai et al. 1995; Loew et al. 1993; Lolkema et al. 1982; Plasek and Hrouda 1991; Ross et al. 2005). For diS-C_3(3) assays relying on the spectral unmixing of free- and bound-dye contributions from complex fluorescence spectra of cell suspensions it is essential to use dye concentrations low enough to guarantee that the amount of intracellular bound dye is directly proportional to the intracellular free dye concentration resulting from the Nernstian accumulation of diS-C_3(3) in the cells (Plasek et al. 1994), see Methods.

Moreover, we will assume that the complex fluorescence of diS-C_3(3) stained cell suspensions is dominated by the fluorescence of free dye dissolved in the cell suspension medium, F_f, and the fluorescence of dye molecules bound to cytosolic proteins, or other intracellular substances, F_b, while both the contribution of fluorescence of unbound dye molecules present in the cell cytosol, F_{in}, and fluorescence of dye molecules bound to the outer cell surface, F_b^{out}, is negligible in properly designed experiments. In particular, F_{in} is negligible compared to F_f if the partial volume of cells in measured suspensions is sufficiently low, what is the case in present experimental protocols. The amount of dye bound to the outer cell surface can also be neglected compared to the amount of the dye bound to cytosolic proteins. This was proved by fluorescence microscopy, which revealed no bright rim around the fluorescent images of stained cells.

Then, following the model presented in (Plasek et al. 1994), the ratio of bound and free-dye fluorescence intensities measured with spectral unmixing, i.e., F_b and F_f, respectively, can be combined with the Nernst equation to yield

$$\frac{F_b}{F_f} = \frac{V_c Q_b S_b k_b}{V_s Q_f S_f} e^{-\frac{F}{RT}\Delta\Psi} = K_{bf} e^{-\frac{\Delta\Psi}{U_{RTF}}} \qquad \text{(A1)}$$

where the physical constants R, T and F have their usual meaning, $\Delta\Psi$ denotes the membrane potential. A number of multiplicative factors involved in this equation represents following experimental parameters: partial volume of cells (V_c) and cell suspension medium (V_s) within an effective fluorescence detection volume inside a cuvette, fluorescence quantum yields (Q_b and Q_f) and instrument sensitivity factors (S_b and S_f) of bound and free-dye fluorescence, respectively, and k_b is a proportionality constant of the ratio between the bound and free-dye concentrations inside the cells. For simplicity, the pre-exponential fraction in Eq. A1 can be represented by a single constant K_{bf}. To highlight quantitative aspects of this equation, we have introduced a voltage factor U_{RTF} = RT/F, the value of which is 25.7–26.9 mV at physiological temperatures between 25 and 37 °C.

Despite the impossibility to determine the actual value of the K_{bf} coefficient in real experiments Eq. A1 can be still used for the assessment of membrane potential differences in certain defined situations. In particular, this is the case, when it is justified to postulate that the cell-related parameters V_c and k_b remain constant on going from a cell physiological state 1 (characterized by membrane potential $\Delta\Psi_1$) to another state 2 (characterized by membrane potential $\Delta\Psi_2$). Upon a simple logarithmic transformation of Eq. A1 we get finally

$$\Delta\Psi_1 = -2.3U_{RTF}\left[\log\frac{F_{b1}}{F_{f1}} - \log K_{bf}\right] \tag{A2a}$$

$$\Delta\Psi_2 = -2.3U_{RTF}\left[\log\frac{F_{b2}}{F_{f2}} - \log K_{bf}\right] \tag{A2b}$$

These two equations can be combined into the following simple formula, in which the unknown constant K_{bf} has been cancelled out:

$$\Delta\Psi_1 - \Delta\Psi_2 = -2.3U_{RTF}\left[\log\frac{F_{b2}}{F_{f2}} - \log\frac{F_{b1}}{F_{f1}}\right] \tag{A3}$$

In this way, the F_b/F_f fluorescence ratios obtained by the spectral unmixing of diS-C_3(3) fluorescence spectra measured in cell suspensions can be used to quantify membrane potential differences in the absolute scale of mV, without necessity to perform any a priori calibration experiment.

However, the Eq. A3 is obviously an oversimplification aimed merely to illustrate the idea of a quantitative link between the diS-C_3(3) fluorescence spectra and membrane potential changes of examined cells. To match real experimental conditions, the above model must be amended by including i) the uptake of diS-C_3(3) by mitochondria, ii) the effect of yeast cell wall and surface potential, and iii) the extrusion of diS-C_3(3) from yeast cells by MDR pumps, responsible for multi drug resistance of yeast cells.

Contribution of probe accumulation in mitochondria

The treatment of the contribution of mitochondria to the diS-C_3(3) accumulation in yeast cell follows also the model already used for animal cells (Plasek et al. 1994), which leads to a conclusion that the correction of Eq. A1 for the contribution of mitochondria can be represented by a multiplicative factor $M(V_m, \Delta\Psi_m)$, which is the function of both the partial volume of mitochondria in cells, V_m, and mitochondrial membrane potential, $\Delta\Psi_m$.

$$\frac{F_b}{F_f} = K_{bf}M(V_m, \Delta\Psi_m)e^{-\frac{\Delta\Psi}{U_{RTF}}} \tag{A4}$$

This means that Eq. A3 can be still used for assessment of membrane potential differences whenever the postulation is justified that neither the partial volume of mitochondria in the cells, nor the mitochondrial membrane potential vary in the course of the experiment. The role of mitochondria-related artefacts in membrane potential assays can also be significantly lessened by working with fermenting yeast cells in which the function of the mitochondria is highly reduced (Criddle and Schatz 1969). On the other hand, experimental protocols based on uncoupling yeast mitochondria with protonophores are not recommended since these protonophores, such as carbonyl cyanide m-chlorophenylhydrazone (CCCP), collapse inevitably the proton electrochemical gradient across the plasma membrane as well (Macey et al. 1978; Pereira et al. 2008; Stevens and Nichols 2007).

The role of cell wall and surface potential

The effect of cell wall, which is specific for yeast and bacteria, has not been treated in models published in our preceding papers. Since the cell wall space of yeast possess negative Donnan potential, a correction should be made for the accumulation of cationic species in the close proximity of cell membrane (Borst-Pauwels 1989; Theuvenet and Borst_Pauwels 1983), albeit under some conditions the role of cation accumulation in the cell wall might be rather small (Gage et al. 1985).

As the Nernstian accumulation of diS-C_3(3) in yeast cells is concerned, a true dye concentration at the periplasm/plasmalemma interface, c_{ppi}, must be therefore inserted into the Nernst equation instead of its bulk concentration, c_{out}, in the cell suspension medium. The former concentration is proportional to the bulk diS-C_3(3) concentration through two distinct exponential factors that arise from i) the partition coefficient of diS-C_3(3) between the aqueous suspension medium and the less polar cell wall space, and ii) the series of Boltzmann equilibriums related to the Donnan potential of cell wall and the surface potential of plasmalemma. It seems therefore practical to introduce a certain "effective"negative surface potential ψ^*, which makes it possible to express the increase of local diS-C_3(3) concentration at membrane surface c_{ppi} with respect to its bulk value c_{out} in terms of a product $c_{out}\exp(\psi^*/U_{RTF})$. Then the Nernst equation used to describe the accumulation of diS-C_3(3) in animal cells (Plasek et al. 1994), i.e.,

$$c_{in} = c_{out}e^{-\frac{F}{RT}\Delta\Psi} \tag{A5}$$

must be replaced by

$$c_{in} = c_{out}e^{-\frac{F}{RT}\psi^*}e^{-\frac{F}{RT}\Delta\Psi}, \tag{A6}$$

and Eq. A3 modified accordingly to yield a following equation

$$-2.3U_{RTF}\left[\log\frac{F_{b2}}{F_{f2}}-\log\frac{F_{b1}}{F_{f1}}\right]=\Delta\Psi_2-\Delta\Psi_1+\left[\psi_2^*-\psi_1^*\right], \quad (A7)$$

which reflects a fact that the intracellular accumulation of small lipophilic cations does not respond correctly to membrane potential changes if the surface potential of examined cells varies in the course of the experiment. This is a very important, thought often ignored, aspect of monitoring cell membrane potentials by using lipophilic cations. In particular, the use of different buffers may result in serious discrepancies between diS-C_3(3) fluorescence intensities measured in apparently parallel assays, just because the surface potential of cell membranes is extremely sensitive to the ionic strength of cell suspension medium. On the other hand, when the ionic strength is maintained constant during the experiment, [$\psi 2^*-\ \psi 1^*$] becomes zero and thus can be omitted

Contribution of MDR pumps

Voltage-sensing fluorescent dyes are possible substrates of MDR pumps responsible for multi drug resistance of yeast cells. When considering the effect of these pumps on dye redistribution it is necessary to move from the thermodynamic equilibrium model to a steady-state equilibrium, under which the dye uptake by cells is counter balanced by the MDR pump mediated outward flux J_{MDR} (in mol m^{-1} s^{-1}). The transmembrane inward flux of ions J (in mol m^{-1} s^{-1}) that is driven by the membrane potential can be expressed

$$J=\frac{G}{zF}\left(U_{RTF}\ln\frac{c_{out}}{c_{in}}-\Delta\Psi\right) \quad (A8)$$

where G is the membrane conductivity, z the ion valence, and other symbols as above (Friedman 2008). In the steady state this flux is offset by J_{MDR}, so that J = J_{MDR}. Under these circumstances Eq. A8 should be replaced by the following formula

$$-2.3U_{RTF}\log\frac{c_{out}}{c_{in}}=\Delta\Psi-\frac{zF}{G}J_{MDR} \quad (A9)$$

This implicates that the cationic dye redistribution reflects false membrane potentials that are reduced with respect to their true values by a term $\Delta\Psi^{MDR}=\frac{zF}{G}J_{MDR}$ and thus, Eq. A3 must be extended to a more complex formula

$$-2.3U_{RTF}\left[\log\frac{F_{b2}}{F_{f2}}-\log\frac{F_{b1}}{F_{f1}}\right]=\Delta\Psi_2-\Delta\Psi_1-\left[\Delta\Psi_2^{MDR}-\Delta\Psi_1^{MDR}\right] \quad (A10)$$

Unfortunately, little is known about the size of MDR mediated currents. This hampers both the qualitative and quantitative evaluation of the membrane potential dependent response of slow dyes. Therefore, Eq. A10 can be used for the assessment of membrane potential changes only in a few special cases, such as when working with MDR pump-deficient yeast mutants and/or with cells for which it was demonstrated that the actual contribution of MDR pumps to membrane potential, $\Delta\Psi^{MDR}$, stays constant and independent of the rate of diS-C_3(3) accumulation in cells (see Methods). Under the latter conditions, the term $\left(\Delta\Psi_2^{MDR}-\Delta\Psi_1^{MDR}\right)$ of Eq. A10 is cancelled out and thus, true $\Delta\Psi_2$ – $\Delta\Psi_1$ differences can be obtained.

Important protocol requirements for quantifying membrane potential changes

The most important requirements for the quantitative evaluation of diS-C_3(3) fluorescence response to membrane potential changes in mV are:

a) It is essential to use dye concentrations low enough to guarantee direct proportionality between the amount of intracellular bound dye and the intracellular free dye concentration resulting from the Nernstian accumulation of diS-C_3(3) in the cells.
b) Any experimental protocol aimed at the assessment of membrane potential changes between two physiological states of examined cell suspension must guarantee that the steady-state dye redistribution between cells and their medium was reached. This does not apply when the time-course of membrane potential changes is monitored.
c) All details of the experiment must be carefully controlled so that no variations occur in the density of cells in cell suspension or in ionic strength of the suspension medium.
d) Ideal situation for the quantitative evaluation of diS-C_3(3) fluorescence in terms of underlying membrane potential changes is represented by experiments in which the cells respond to any stimulus in periods short enough from the point of view of possible changes in cellular parameters such as metabolism, protein synthesis, macromolecular composition of cytosol as well as partial volume of mitochondria and mitochondrial membrane potential.

References

Bakker R, Dobbelmann J, Borst-Pauwels GWFH (1986) Membrane potential in the yeast Endomyces magnusii measured by microelectrodes and TPP+ distribution. Biochim Biophys Acta 861:205–209

Bashford CL (1981) The measurement of membrane potential using optical indicators. Biosci Rep 1:183–196

Borst-Pauwels GWFH (1989) Ion transport in yeast including lipophilic ions. Methods Enzymol 174:603–616

Cohen LB, Salzberg BM (1978) Optical measurement of membrane potential. Rev Physiol Biochem Pharmacol 83:35–88

Cossarizza A, Ceccarelli D, Masini A (1996) Functional heterogeneity of an isolated mitochondrial population revealed by cytofluorometric analysis at the single organelle level. Exp Cell Res 222:84–94

Criddle RS, Schatz G (1969) Promitochondria of anaerobically grown yeast. I. Isolation and biochemical properties. Biochemistry 8:322–334

Ehrenberg B, Montana V, Wei MD, Wuskell JP, Loew LM (1988) Membrane potential can be determined in individual cells from the nernstian distribution of cationic dyes. Biophys J 53:785–794

Freedman JC, Hoffman JF (1979) The relation between dicarbocyanine dye fluorescence and the membrane potential of human red blood cells set at varying Donnan equilibria. J Gen Physiol 74:187–212

Friedman MH (2008) Principles and models of biological transport. Springer, New York, p 508

Gage RA, Vanwijngaarden W, Theuvenet APR, Borst-Pauwels GWFH, Verkleij AJ (1985) Inhibition of Rb+ uptake in yeast by Ca2+ is caused by a reduction in the surface potential and not in the Donnan potential. Biochim Biophys Acta 812:1–8

Gaskova D, Brodska B, Herman P et al (1998) Fluorescent probing of membrane potential in walled cells: diS-C-3(3) assay in Saccharomyces cerevisiae. Yeast 14:1189–1197

Gross D, Loew LM (1989) Fluorescent indicators of membrane potential: microspectrofluorometry and imaging. Methods Cell Biol 30:193–218

Hauer R, Hofer M (1978) Evidence for interactions between the energy-dependent transport of sugars and the membrane potential in the yeast Rhodotorula gracilis (Rhodosporidium toruloides). J Membr Biol 43:335–349

Hauer R, Uhlemann G, Neumann J, Hofer M (1981) Proton pumps of the plasmalemma of the yeast Rhodotorula gracilis—their coupling to fluxes of potassium and other ions. Biochim Biophys Acta 649:680–690

Hladky SB, Rink TJ (1976) Potential difference and the distribution of ions across the human red blood cell membrane; a study of the mechanism by which the fluorescent cation, diS-C3-(5) reports membrane potential. J Physiol 263:287–319

Hockings PD, Rogers PJ (1996) The measurement of transmembrane electrical potential with lipophilic cations. Biochim Biophys Acta 1282:101–106

Hofer M, Kunemund A (1985) Tetraphenylphosphonium ion is a true indicator of negative plasma-membrane potential in the yeast Rhodotorula glutinis. Experiments under osmotic stress and at low external pH values. Biochem J 225:815–819

Hofer M, Novacky A (1986) Measurement of plasma membrane potentials of yeast cells with glass microelectrodes. Biochim Biophys Acta 862:372–378

Hofer M, Nicolay K, Robillard G (1985) The electrochemical H^+ gradient in the yeast Rhodotorula glutinis. J Bioenerg Biomem 17:175–182

Hoffman JF, Laris PC (1974) Determination of membrane potentials in human and Amphiuma red blood cells by means of a fluorescent probe. J Physiol 239:519–552

Kaji DM (1993) Effect of membrane potential on K-Cl transport in human erythrocytes. Am J Physiol 239(264):C376–C382

Krasznai Z, Marian T, Balkay L, Emri M, Tron L (1995) Flow cytometric determination of absolute membrane potential of cells. J Photochem Photobiol B 28:93–99

Labajova A, Vojtiskova A, Krivakova P, Kofranek J, Drahota Z, Houstek J (2006) Evaluation of mitochondrial membrane potential using a computerized device with a tetraphenylphosphonium-selective electrode. Anal Biochem 353:37–42

Ling G, Gerard RW (1949) The normal membrane potential of frog Sartorius fibers. J Cell Compart Physiol 34:383–396

Lloyd JBF (1971) Synchronized excitation of fluorescence emission spectra. Nat Phys Sci 231:64–65

Loew LM, Tuft RA, Carrington W, Fay FS (1993) Imaging in five dimensions: time-dependent membrane potentials in individual mitochondria. Biophys J 65:2396–2407

Lolkema JS, Hellingwerf KJ, Konings WN (1982) The effect of 'probe binding' on the quantitative determination of the proton-motive force in bacteria. Biochim Biophys Acta 681:85–94

Macey RI, Adorante JS, Orme FW (1978) Erythrocyte membrane potentials determined by hydrogen ion distribution. Biochim Biophys Acta 512:284–295

Mao C, Kisaalita WS (2004) Determination of resting membrane potential of individual neuroblastoma cells (IMR-32) using a potentiometric dye (TMRM) and confocal microscopy. J Fluoresc 14:739–743

Maresova L, Urbankova E, Gaskova D, Sychrova H (2006) Measurements of plasma membrane potential changes in Saccharomyces cerevisiae cells reveal the importance of the Tok1 channel in membrane potential maintenance. FEMS Yeast Res 6:1039–1046

Maresova L, Muend S, Zhang YQ, Sychrova H, Rao R (2009) Membrane hyperpolarization drives cation influx and fungicidal activity of amiodarone. J Biol Chem 284:2795–2802

Pena A, Sanchez NS, Calahorra M (2010) Estimation of the electric plasma membrane potential difference in yeast with fluorescent dyes: comparative study of methods. J Bioenerg Biomem 42:419–432

Pereira MBP, Tisi R, Fietto LG et al (2008) Carbonyl cyanide m-chlorophenylhydrazone induced calcium signaling and activation of plasma membrane H+ -ATPase in the yeast Saccharomyces cerevisiae. FEMS Yeast Res 8:622–630

Plasek J, Hrouda V (1991) Assessment of membrane potential changes using the carbocyanine dye, diS-C_3(5): synchronous excitation spectroscopy studies. Eur Biophys J 19:183–188

Plasek J, Sigler K (1996) Slow fluorescent indicators of membrane potential: a survey of different approaches to probe response analysis. J Photochem Photobiol B 33:101–124

Plasek J, Dale RE, Sigler K, Laskay G (1994) Transmembrane potentials in cells: a diS-C_3(3) assay for relative potentials as an indicator of real changes. Biochim Biophys Acta 1196:181–190

Plasek J, Gaskova D, Vecer J, Sigler K (2000) Use of synchronously excited fluorescence to assess the accumulation of membrane potential probes in yeast cells. Folia Microbiol 45:225–229

Przybylo M, Borowik T, Langner M (2010) Fluorescence techniques for determination of the membrane potentials in high throughput screening. J Fluoresc 20:1139–1157

Ross MF, Kelso GF, Blaikie FH et al (2005) Lipophilic triphenylphosphonium cations as tools in mitochondrial bioenergetics and free radical biology. Biochemistry (Mosc) 70:222–230

Shapiro HM (1994) Cell membrane potential analysis. Methods Cell Biol 41:121–133

Sims PJ, Waggoner AS, Wang CH, Hoffman JF (1974) Studies on the mechanism by which cyanine dyes measure membrane potential

in red blood cells and phosphatidylcholine vesicles. Biochemistry 13:3315–3330

Smith JC (1990) Potential-sensitive molecular probes in membranes of bioenergetic relevance. Biochim Biophys Acta 1016:1–28

Stevens HC, Nichols JW (2007) The proton electrochemical gradient across the plasma membrane of yeast is necessary for phospholipid flip. J Biol Chem 282:17563–17567

Sundelacruz S, Levin M, Kaplan DL (2009) Role of membrane potential in the regulation of cell proliferation and differentiation. Stem Cell Rev 5:231–246

Theuvenet APR, Borst-Pauwels GWFH (1983) Effect of surface potential on Rb + uptake in yeast. The effect of pH. Biochim Biophys Acta 734:62–69

Ullrich WR, Larsson M, Larsson CM, Lesch S, Novacky A (1984) Ammonium uptake in Lemna gibba G 1, related membrane potential changes, and inhibition of anion uptake. Physiol Plant 61:369–376

Waggoner A (1976) Optical probes of membrane potential. J Membr Biol 27:317–334

Waggoner AS (1979) Dye indicators of membrane potential. Annu Rev Biophys Bioeng 8:47–68